Robust Blood Sugar Monitoring in Diabetic Patients with Timing Jitter due to Human Factors

ELI G. PALE-RAMON, JORGE A. ORTEGA-CONTRERAS, KAREN J. URIBE-MURCIA, YURIY S. SHMALIY

Department of Electronics Engineering, Universidad de Guanajuato, Salamanca, 36855, MEXICO

Abstract: Blood sugar monitoring in diabetic patients is commonly provided with timing jitter caused by human factors. In this paper we address the problem by developing the robust H2 optimal finite impulse response (OFIR) filter under under possible disturbances, initial errors, and measurement errors. The filter is applied to data collected daily before breakfast from diabetic patients. It is shown that the robust H2-OFIR filter improves the accuracy of the OFIR filter by the factor of less than the fractional time jitter. That is, for large fractional timing jitter of 10% the improvement would be less than 10% that is small. Otherwise, it is worth using robust estimators.

Keywords: blood sugar level, diabetic patients, timing jitter, robust filter, optimal filter

Received: March 15, 2021. Revised: March 26, 2022. Accepted: April 27, 2022. Published: May 19, 2022.

1. Introduction

Timing jitter occurs in different practical situations for a variety of reasons. The first presentation of the problem was given in [1]. Later, the sampling time jitter was discovered in many practical applications and standardized in [2], [3].

Regular blood sugar monitoring is conducted in diabetic patients to timely reflect the influence of diet, exercise, stress, and drugs on the blood glucose level [4]. This also gives the necessary data for evidenced-based clinical decision-making by healthcare professionals. Monitoring is provided at least once per day for type 2 diabetes and more than 4 times per day for type 1 diabetes [5]. Although glucose monitoring is usually assigned at a certain time, real time may differ by several hours due to human factors – thus random timing jitter. It is worth noting that during glucose measurements, jitter may take several hours [6].

Of importance is that timing jitter does not depend on the sampling interval, is often normally distributed, and makes the model uncertain that requires robust approaches [7]–[9]. The robust H_2 filter has several distinctive features: it becomes the Kalman filter (KF) in white Gaussian environments and gives robust estimates for maximized errors. The H_2 filter appears from the transform domain, where the squared Frobenius norm of the error-to-error transfer function $\mathcal{T}$ is minimized for maximized errors, and the solution can also be found numerically using a linear matrix inequality (LMI) [14]–[17].

The robustness can also be improved using batch finite impulse response (FIR) structures [18], which are bounded input bounded output stable and can work with full (not diagonal) block error matrices and discard errors beyond the averaging horizon. The first receding horizon H_2-FIR filter was developed in [18] for disturbed systems and the envelope-constrained H_2-FIR filter proposed in [19]. Some other FIR solutions can be found in [20]–[24], and it is important that the H_2-FIR filter can be as robust as the H_∞ filter [25]. Even so, the H_2-FIR approach is still poorly developed for uncertain systems, and its robustness to timing jitter still remains unknown.

In this paper, we develop the H_2 optimal FIR (OFIR) filter for blood sugar monitoring in diabetic persons taking into account timing jitter. Based on glucose measurements in diabetic patients, we investigate the effect of timing jitter on the H_2-OFIR filter performance in a comparison with the OFIR filter [26], [27].

2. Model and Problem Formulation

We represent the blood sugar dynamics with a linear time-invariant (LTI) continuous-time state-space equations

$$\frac{\mathrm{d}}{\mathrm{d}t}\mathbf{x}(t) = \mathbf{A}\mathbf{x}(t) + \mathbf{L}\mathbf{w}(t)\,, \quad (1)$$

$$\mathbf{y}(t) = \mathbf{C}\mathbf{x}(t) + \mathbf{v}(t)\,, \quad (2)$$

where $\mathbf{x}(t) \in \mathbb{R}^K$, $\mathbf{y}(t) \in \mathbb{R}^M$, $\mathbf{w}(t) \in \mathbb{R}^P$, and $\mathbf{v}(t) \in \mathbb{R}^M$. The matrices $\mathbf{A} \in \mathbb{R}^{K\times K}$, $\mathbf{L} \in \mathbb{R}^{K\times P}$, and $\mathbf{C} \in \mathbb{R}^{M\times K}$ are constant and known. The glucose measurements are provided with the sampling time $\tau_k = t_k - t_{k-1}$, where k is the discrete-time index. We assume that τ_k is random and uncertain due to human factors. We represent τ_k as $\tau_k = \tau + \tilde{\tau}_k = \tau(1 + \delta_{\tau k})$, where τ is the known mean, $\tilde{\tau}_k$ is the zero mean random jitter, and $\delta_{\tau k} = \frac{\tilde{\tau}_k}{\tau}$ is the fractional jitter.

To go to discrete time, we integrate (1) from t_{k-1} to t_k and write the solution as

$$\mathbf{x}(t_k) = e^{\mathbf{A}\tau_k}\mathbf{x}(t_{k-1}) + \int_{t_{k-1}}^{t_k} e^{\mathbf{A}(t_k-\theta)}\mathbf{L}\mathbf{w}(\theta)\mathrm{d}\theta\,, \quad (3)$$

$$\mathbf{y}(t_k) = \mathbf{C}\mathbf{x}(t_k) + \mathbf{v}(t_k)\,. \quad (4)$$

Substituting $\mathbf{x}_k \cong \mathbf{x}(t_k)$, $\mathbf{y}_k \cong \mathbf{y}(t_k)$, and $\mathbf{v}_k \cong \mathbf{v}(t_k)$ gives

$$\mathbf{x}_k = (\mathbf{F} + \Delta\mathbf{F}_k)\mathbf{x}_{k-1} + (\mathbf{B} + \Delta\mathbf{B}_k)\mathbf{w}_k\,, \quad (5)$$

$$\mathbf{y}_k = \mathbf{H}\mathbf{x}_k + \mathbf{v}_k\,, \quad (6)$$

where $\mathbf{H} = \mathbf{C}$, $\mathbf{F} = e^{\mathbf{A}\tau}$, $\Delta\mathbf{F}_k = e^{\mathbf{A}\tilde{\tau}_k}$, the disturbance $\mathbf{w}_k$ is defined by the stochastic integral

$$\mathbf{B}_k\mathbf{w}_k = \int_{t_{k-1}}^{t_k} e^{\mathbf{A}(t_k-\theta)}\mathbf{L}\mathbf{w}(\theta)\,\mathrm{d}\theta\,,$$

where $\mathbf{B}_k = \mathbf{B} + \Delta\mathbf{B}_k$, and the data error $\mathbf{v}_k = \frac{1}{\tau_k}\int_{t_{k-1}}^{t_k}\mathbf{v}(t)\,\mathrm{d}t$ is supposed to be zero mean and bounded.

For white Gaussian $\mathbf{w}_k \sim \mathcal{N}(\mathbf{0},\mathbf{Q}_k)$, the covariance $\mathbf{Q}_k$ is given by $\mathbf{Q}_k = \mathcal{E}\{\mathbf{w}_k\mathbf{w}_k^T\} \cong \tau_k\mathbf{L}\mathcal{S}_w\mathbf{L}^T$, where $\mathcal{S}_w$ is the power spectral density (PSD) of $\mathbf{w}(t)$, and we maximize it as

$$\bar{\mathbf{Q}} = \frac{\tau + \max|\tilde{\tau}_k|}{\tau}\mathbf{Q} = (1+\bar{\delta}_\tau)\mathbf{Q}\,, \tag{7}$$

where $\mathbf{Q} = \tau\mathbf{L}\mathcal{S}_w\mathbf{L}^T$ and $\bar{\delta}_\tau = \max|\delta_{\tau k}| = \frac{\max|\tilde{\tau}_k|}{\tau}$ is the maximized fractional jitter. For $\mathbf{v}_k \sim \mathcal{N}(\mathbf{0},\mathbf{R}_k)$, the covariance $\mathbf{R}_k = \mathcal{E}\{\mathbf{v}_k\mathbf{v}_k^T\}$ is defined as $\mathbf{R}_k = \frac{1}{\tau_k}\mathcal{S}_v$, where $\mathcal{S}_v$ is the PSD of $\mathbf{v}(t)$, and we similarly have

$$\bar{\mathbf{R}} = \frac{1}{1+\bar{\delta}_\tau}\mathbf{R} \cong (1-\bar{\delta}_\tau)\mathbf{R}\,. \tag{8}$$

3. Extended Model

The robust H_2-OFIR filter can be developed for timing jitter, if we reorganize the model (5) and (6) as

$$\mathbf{x}_k = \mathbf{F}\mathbf{x}_{k-1} + \xi_k\,, \tag{9}$$
$$\mathbf{y}_k = \mathbf{H}\mathbf{x}_k + \mathbf{v}_k\,, \tag{10}$$

where the zero mean error vector ξ_k is given by

$$\xi_k = \Delta\mathbf{F}_k\mathbf{x}_{k-1} + (\mathbf{B}+\Delta\mathbf{B}_k)\mathbf{w}_k\,. \tag{11}$$

Next, we follow [26] and extend (9) and (10) to the averaging horizon $[m,k]$ of N points, where $m = k-N+1$, as

$$\mathbf{X}_{m,k} = \mathbf{F}_N\mathbf{x}_m + \hat{\mathbf{F}}_N\Xi_{m,k}\,, \tag{12}$$
$$\mathbf{Y}_{m,k} = \mathbf{H}_N\mathbf{x}_m + \mathbf{G}_N\Xi_{m,k} + \mathbf{V}_{m,k}\,, \tag{13}$$

where $\mathbf{X}_{m,k} = [\mathbf{x}_m^T\ \mathbf{x}_{m+1}^T \dots \mathbf{x}_k^T]^T$, $\mathbf{Y}_{m,k} = [\mathbf{y}_m^T\ \mathbf{y}_{m+1}^T \dots \mathbf{y}_k^T]^T$, $\Xi_{m,k} = [\xi_m^T\ \xi_{m+1}^T \dots \xi_k^T]^T$, $\mathbf{V}_{m,k} = [\mathbf{v}_m^T\ \mathbf{v}_{m+1}^T \dots \mathbf{v}_k^T]^T$, and the partitioned matrices are

$$\mathbf{F}_N = \begin{bmatrix}\mathbf{I} & \mathbf{F}^T & \dots & \mathbf{F}^{N-2^T} & \mathbf{F}^{N-1^T}\end{bmatrix}^T, \tag{14}$$

$$\hat{\mathbf{F}}_N = \begin{bmatrix} \mathbf{I} & \mathbf{0} & \dots & \mathbf{0} & \mathbf{0} \\ \mathbf{F} & \mathbf{I} & \dots & \mathbf{0} & \mathbf{0} \\ \vdots & \vdots & \ddots & \vdots & \vdots \\ \mathbf{F}^{N-2} & \mathbf{F}^{N-3} & \dots & \mathbf{I} & \mathbf{0} \\ \mathbf{F}^{N-1} & \mathbf{F}^{N-2} & \dots & \mathbf{F} & \mathbf{I} \end{bmatrix}, \tag{15}$$

$\mathbf{H}_N = \bar{\mathbf{H}}_N\mathbf{F}_N$, $\mathbf{G}_N = \bar{\mathbf{H}}_N\hat{\mathbf{F}}_N$, and $\bar{\mathbf{H}}_N = \mathrm{diag}(\underbrace{\mathbf{H}\,\mathbf{H}\dots\mathbf{H}}_{N})$.

The extended uncertain vector Ξ_k is

$$\Xi_{m,k} = \mathbf{F}_{m,k}^{\Delta}\mathbf{x}_m + (\bar{\mathbf{B}}_N + \mathbf{D}_{m,k}^{\Delta})\mathbf{W}_{m,k}\,, \tag{16}$$

where $\bar{\mathbf{B}}_N = \mathrm{diag}(\underbrace{\mathbf{B}\,\mathbf{B}\dots\mathbf{B}}_{N})$, $\mathbf{F}_{m,k}^{\Delta}$ and $\mathbf{D}_{m,k}^{\Delta}$ are given by

$$\mathbf{F}_{m,k}^{\Delta} = \begin{bmatrix} \mathbf{0} \\ \Delta\mathbf{F}_{m+1} \\ \vdots \\ \Delta\mathbf{F}_{k-1}\tilde{\mathcal{F}}_{k-2}^{m+1} \\ \Delta\mathbf{F}_k\tilde{\mathcal{F}}_{k-1}^{m+1} \end{bmatrix}, \tag{17}$$

$$\mathbf{D}_{m,k}^{\Delta} = \begin{bmatrix} \mathbf{0} & \mathbf{0} & \dots & \mathbf{0} & \mathbf{0} \\ \Delta\mathbf{F}_{m+1} & \mathbf{0} & \dots & \mathbf{0} & \mathbf{0} \\ \vdots & \vdots & \ddots & \vdots & \vdots \\ \Delta\mathbf{F}_{k-1}\tilde{\mathcal{F}}_{k-2}^{m+1} & \Delta\mathbf{F}_{k-1}\tilde{\mathcal{F}}_{k-2}^{m+2} & \dots & \mathbf{0} & \mathbf{0} \\ \Delta\mathbf{F}_k\tilde{\mathcal{F}}_{k-1}^{m+1} & \Delta\mathbf{F}_k\tilde{\mathcal{F}}_{k-1}^{m+2} & \dots & \Delta\mathbf{F}_k & \mathbf{0} \end{bmatrix}, \tag{18}$$

and matrix $\tilde{\mathcal{F}}_r^g$ of uncertain products is specified as

$$\tilde{\mathcal{F}}_r^g = \begin{cases} \mathbf{F}_r^u\mathbf{F}_{r-1}^u\dots\mathbf{F}_g^u\,, & g < r+1\,, \\ \mathbf{I}\,, & g = r+1 \\ \mathbf{0}\,, & g > r+1 \end{cases}. \tag{19}$$

Finally, we write the extended state equation as

$$\mathbf{X}_{m,k} = (\mathbf{F}_N + \tilde{\mathbf{F}}_{m,k})\mathbf{x}_m + (\hat{\mathbf{F}}_N + \tilde{\mathbf{D}}_{m,k})\mathbf{W}_{m,k}\,, \tag{20}$$

where $\tilde{\mathbf{F}}_{m,k} = \hat{\mathbf{F}}_N\mathbf{F}_{m,k}^{\Delta}$ and $\tilde{\mathbf{D}}_{m,k} = \hat{\mathbf{F}}_N\mathbf{D}_{m,k}^{\Delta}$. The state $\mathbf{x}_k$ can now be taken as the last row vector in (20),

$$\mathbf{x}_k = (\mathbf{F}^{N-1} + \bar{\tilde{\mathbf{F}}}_{m,k})\mathbf{x}_m + (\bar{\hat{\mathbf{F}}}_N + \bar{\tilde{\mathbf{D}}}_{m,k})\mathbf{W}_{m,k}\,, \tag{21}$$

where $\bar{\tilde{\mathbf{F}}}_{m,k}$, $\bar{\hat{\mathbf{F}}}_N$, and $\bar{\tilde{\mathbf{D}}}_{m,k}$ are the last row vectors in $\tilde{\mathbf{F}}_{m,k}$, $\hat{\mathbf{F}}_N$, and $\tilde{\mathbf{D}}_{m,k}$, respectively.

Similarly, we obtain the extended observation equation

$$\mathbf{Y}_{m,k} = (\mathbf{H}_N + \tilde{\mathbf{H}}_{m,k})\mathbf{x}_m + (\mathbf{G}_N + \tilde{\mathbf{T}}_{m,k})\mathbf{W}_{m,k} + \mathbf{V}_{m,k}, \tag{22}$$

where $\tilde{\mathbf{H}}_{m,k} = \mathbf{M}_N\mathbf{F}_{m,k}^{\Delta}$, $\tilde{\mathbf{T}}_{m,k} = \mathbf{M}_N\mathbf{D}_{m,k}^{\Delta}$, and $\mathbf{M}_N = \bar{\mathbf{H}}_N\hat{\mathbf{F}}_N$.

4. Robust H$_2$-Ofir Filter

The FIR filtering estimate can be defined as [23]

$$\begin{aligned}\hat{\mathbf{x}}_k &= \mathcal{H}_N\mathbf{Y}_{m,k} \\ &= \mathcal{H}_N(\mathbf{H}_N + \tilde{\mathbf{H}}_{m,k})\mathbf{x}_m + \mathcal{H}_N\mathbf{V}_{m,k} \\ &\quad + \mathcal{H}_N(\mathbf{G}_N + \tilde{\mathbf{T}}_{m,k})\mathbf{W}_{m,k}\,,\end{aligned} \tag{23}$$

where $\mathcal{H}_N$ is the filter gain, and $\tilde{\mathbf{H}}_{m,k}$ and $\tilde{\mathbf{T}}_{m,k}$ are uncertain matrices specified after (22). The unbiasedness condition $\mathcal{E}\{\hat{\mathbf{x}}_k\} = \mathcal{E}\{\mathbf{x}_k\}$ applied to (21) and (23) gives the unbiasedness constrain

$$\mathbf{F}^{N-1} = \mathcal{H}_N\mathbf{H}_N\,, \tag{24}$$

and the estimation error $\varepsilon_k = \mathbf{x}_k - \hat{\mathbf{x}}_k$ can be written as

$$\begin{aligned}\varepsilon_k &= (\mathbf{F}^{N-1} - \mathcal{H}_N\mathbf{H}_N + \bar{\tilde{\mathbf{F}}}_{m,k} - \mathcal{H}_N\tilde{\mathbf{H}}_{m,k})\mathbf{x}_m \\ &\quad + (\bar{\hat{\mathbf{F}}}_N - \mathcal{H}_N\mathbf{G}_N + \bar{\tilde{\mathbf{D}}}_{m,k} - \mathcal{H}_N\tilde{\mathbf{T}}_{m,k})\mathbf{W}_{m,k} \\ &\quad - \mathcal{H}_N\mathbf{V}_{m,k}\,.\end{aligned} \tag{25}$$

Next, we generalize ε_k in the form

$$\begin{aligned}\varepsilon_k &= (\mathcal{B}_N + \tilde{\mathcal{B}}_{m,k})\mathbf{x}_m + (\mathcal{W}_N + \tilde{\mathcal{W}}_{m,k})\mathbf{W}_{m,k} \\ &\quad -\mathcal{V}_N \mathbf{V}_{m,k}\,, \end{aligned} \quad (26)$$

where $\mathcal{B}_N = \mathbf{F}^{N-1} - \mathcal{H}_N \mathbf{H}_N$, $\mathcal{W}_N = \bar{\bar{\mathbf{F}}}_N - \mathcal{H}_N \mathbf{G}_N$, and $\mathcal{V}_N = \mathcal{H}_N$, $\tilde{\mathcal{B}}_{m,k} = \bar{\tilde{\mathbf{F}}}_{m,k} - \mathcal{H}_N \tilde{\mathbf{H}}_{m,k}$ and $\tilde{\mathcal{W}}_{m,k} = \bar{\tilde{\mathbf{D}}}_{m,k} - \mathcal{H}_N \tilde{\mathbf{T}}_{m,k}$. This generalises (26) as

$$\varepsilon_k = \bar{\varepsilon}_{xk} + \bar{\varepsilon}_{wk} + \bar{\varepsilon}_{vk} + \tilde{\varepsilon}_{xk} + \tilde{\varepsilon}_{wk}\,, \quad (27)$$

where the sub errors are defined as

$$\begin{aligned}\bar{\varepsilon}_{xk} &= \mathcal{B}_N \mathbf{x}_m\,, \quad \bar{\varepsilon}_{wk} = \mathcal{W}_N \mathbf{W}_{m,k}\,, \\ \bar{\varepsilon}_{vk} &= -\mathcal{V}_N \mathbf{V}_{m,k}\,, \\ \tilde{\varepsilon}_{xk} &= \tilde{\mathcal{B}}_{m,k}\mathbf{x}_m\,, \quad \tilde{\varepsilon}_{wk} = \tilde{\mathcal{W}}_{m,k}\mathbf{W}_{m,k}\,. \end{aligned} \quad (28)$$

We now have five sub transfer functions: $\mathcal{T}_{\bar{x}}(z)$ for ε_x-to-$\bar{\varepsilon}_x$, $\mathcal{T}_{\bar{w}}(z)$ for ε_w-to-$\bar{\varepsilon}_w$, $\mathcal{T}_{\bar{v}}(z)$ for ε_v-to-$\bar{\varepsilon}_v$, $\mathcal{T}_{\tilde{x}}(z)$ for ε_x-to-$\tilde{\varepsilon}_x$, and $\mathcal{T}_{\tilde{w}}(z)$ for ε_w-to-$\tilde{\varepsilon}_w$, and can proceed with the derivation of the batch H_2-OFIR filter.

4.1 Batch H_2-Ofir Filter

To derive the batch H_2-OFIR filter, we need a lemma.

Lemma 1: Given the model (9) and (10), Then the ξ-to-$\mathbf{y}$ transfer function on $[m,k]$ is $\mathcal{T}(z) = \mathbf{C}_w(\mathbf{I}z - \mathbf{A}_w)^{-1} z\mathbf{B}_w$, where the strictly sparse matrices $\mathbf{A}_w$ and $\mathbf{B}_w$ are defined as

$$\mathbf{A}_w = \begin{bmatrix} \mathbf{0} & \mathbf{I} & \mathbf{0} & \dots & \mathbf{0} \\ \mathbf{0} & \mathbf{0} & \mathbf{I} & \dots & \mathbf{0} \\ \vdots & \vdots & \vdots \ddots & \vdots & \\ \mathbf{0} & \mathbf{0} & \mathbf{0} & \dots & \mathbf{I} \\ \mathbf{0} & \mathbf{0} & \mathbf{0} & \dots & \mathbf{0} \end{bmatrix}, \quad \mathbf{B}_w = \begin{bmatrix} \mathbf{0} \\ \mathbf{0} \\ \vdots \\ \mathbf{0} \\ \mathbf{I} \end{bmatrix} \quad (29)$$

and $\mathbf{C}_w$ is a real matrix. The squared Frobenius norm of the weighted transfer function $\bar{\mathcal{T}}(z)$ is

$$\begin{aligned}\|\bar{\mathcal{T}}(z)\|_F^2 &= \frac{1}{2\pi}\int_0^{2\pi} \mathrm{tr}\,[\mathcal{T}(e^{j\omega T})\Xi\mathcal{T}^*(e^{j\omega T})]\,\mathrm{d}\omega T \quad (30) \\ &= \mathrm{tr}(\mathbf{C}_w \Xi \mathbf{C}_w^T)\,, \quad (31)\end{aligned}$$

where $\mathcal{T}^*$ is complex conjugate of $\mathcal{T}$ and Ξ is a symmetric positive definite weighting matrix.

Proof: The proof can be found in [31]. ∎

Using lemma 1 and introducing $\chi_m = \mathcal{E}\{\mathbf{x}_m \mathbf{x}_m^T\}$, $\mathcal{Q}_N = \mathcal{E}\{\mathbf{W}_{m,k}\mathbf{W}_{m,k}^T\}$, and $\mathcal{R}_N = \mathcal{E}\{\mathbf{V}_{m,k}\mathbf{V}_{m,k}^T\}$, we obtain the squared Frobenius norms $\|\bar{\mathcal{T}}_{\bar{x}}(z)\|_F^2 = \mathrm{tr}(\mathcal{B}_N \chi_m \mathcal{B}_N^T)$, $\|\bar{\mathcal{T}}_{\bar{w}}(z)\|_F^2 = \mathrm{tr}(\mathcal{W}_N \mathcal{Q}_N \mathcal{W}_N^T)$, and $\|\bar{\mathcal{T}}_{\bar{v}}(z)\|_F^2 = \mathrm{tr}(\mathcal{V}_N \mathcal{R}_N \mathcal{V}_N^T)$. For ε_x-to-$\tilde{\varepsilon}_x$, we obtain

$$\begin{aligned}\|\bar{\mathcal{T}}_{\tilde{x}}(z)\|_F^2 = \tilde{\chi}_m^F &= \mathrm{tr}\mathcal{E}\{\tilde{\mathcal{B}}_{m,k}\mathbf{x}_m\mathbf{x}_m^T\tilde{\mathcal{B}}_{m,k}^T\} \\ &= \mathrm{tr}\mathcal{E}\{\bar{\tilde{\mathbf{F}}}_{m,k}\mathbf{x}_m\mathbf{x}_m^T\bar{\tilde{\mathbf{F}}}_{m,k}^T\}\,, \end{aligned} \quad (32)$$

and, for ε_w-to-$\tilde{\varepsilon}_w$, we have

$$\begin{aligned}\|\bar{\mathcal{T}}_{\tilde{w}}(z)\|_F^2 &= \mathrm{tr}\,\mathcal{E}\{\tilde{\mathcal{W}}_{m,k}\mathbf{W}_{m,k}\mathbf{W}_{m,k}^T\tilde{\mathcal{W}}_{m,k}^T\} \\ &= \mathrm{tr}(\tilde{\mathbf{Q}}_N^D - \tilde{\mathbf{Q}}_N^{DT}\mathcal{H}_N^T - \mathcal{H}_N\tilde{\mathbf{Q}}_N^{TD} \\ &\quad + \mathcal{H}_N\tilde{\mathbf{Q}}_N^T\mathcal{H}_N^T)\,, \end{aligned} \quad (33)$$

where $\tilde{\mathbf{Q}}_N^D = \mathcal{E}\{\bar{\tilde{\mathbf{D}}}_{m,k}\mathbf{W}_{m,k}\mathbf{W}_{m,k}^T\bar{\tilde{\mathbf{D}}}_{m,k}^T\}$, $\tilde{\mathbf{Q}}_N^{DT} = \mathcal{E}\{\bar{\tilde{\mathbf{D}}}_{m,k}\mathbf{W}_{m,k}\mathbf{W}_{m,k}^T\tilde{\mathbf{T}}_{m,k}^T\}$, $\tilde{\mathbf{Q}}_N^{TD} = \mathcal{E}\{\tilde{\mathbf{T}}_{m,k}\mathbf{W}_{m,k}\mathbf{W}_{m,k}^T\bar{\tilde{\mathbf{D}}}_{m,k}^T\}$, and $\tilde{\mathbf{Q}}_N^T = \mathcal{E}\{\tilde{\mathbf{T}}_{m,k}\mathbf{W}_{m,k}\mathbf{W}_{m,k}^T\tilde{\mathbf{T}}_{m,k}^T\}$.

The following theorem states the batch *a posteriori* H_2-OFIR filter for data with timing jitter.

Theorem 1: Given model (21) and (22) with zero mean and mutually uncorrelated timing jitter and other errors. The batch a posteriori H_2-OFIR filtering estimate $\hat{\mathbf{x}}_k = \mathcal{H}_N \mathbf{Y}_{m,k}$ specified by (23) has the gain

$$\begin{aligned}\mathcal{H}_N &= (\mathbf{F}^{N-1}\chi_m\mathbf{H}_N^T + \alpha_\tau\bar{\bar{\mathbf{F}}}_N\mathcal{Q}_N\mathbf{G}_N^T + \tilde{\mathbf{Q}}_N^{DT}) \\ &\quad \times(\mathbf{H}_N\chi_m\mathbf{H}_N^T + \alpha_\tau\mathbf{G}_N\mathcal{Q}_N\mathbf{G}_N^T \\ &\quad + \beta_\tau\mathcal{R}_N + \tilde{\mathbf{Q}}_N^T)^{-1}\,, \end{aligned} \quad (34)$$

where $\alpha_\tau = 1 + \bar{\delta}_\tau$, $\beta_\tau = 1 - \bar{\delta}_\tau$, and $\bar{\delta}_\tau$.

Proof: Consider (27) and represent the trace $\mathrm{tr}\mathbf{P} = \{\varepsilon_k^T\varepsilon_k\}$ of the error matrix $\mathbf{P}$ as

$$\begin{aligned}\mathrm{tr}\,\mathbf{P} &= \mathcal{E}\{(\bar{\varepsilon}_{xk} + \bar{\varepsilon}_{wk} + \bar{\varepsilon}_{vk} + \tilde{\varepsilon}_{xk} + \tilde{\varepsilon}_{wk})^T(\dots)\} \\ &= \mathcal{E}\{\bar{\varepsilon}_{xk}^T\bar{\varepsilon}_{xk}\} + \mathcal{E}\{\bar{\varepsilon}_{wk}^T\bar{\varepsilon}_{wk}\} + \mathcal{E}\{\bar{\varepsilon}_{vk}^T\bar{\varepsilon}_{vk}\} \\ &\quad + \mathcal{E}\{\tilde{\varepsilon}_{xk}^T\tilde{\varepsilon}_{xk}\} + \mathcal{E}\{\tilde{\varepsilon}_{wk}^T\tilde{\varepsilon}_{wk}\} \\ &= \|\bar{\mathcal{T}}_{\bar{x}}(z)\|_F^2 + \|\bar{\mathcal{T}}_{\bar{w}}(z)\|_F^2 + \|\bar{\mathcal{T}}_{\bar{v}}(z)\|_F^2 \\ &\quad + \|\bar{\mathcal{T}}_{\tilde{x}}(z)\|_F^2 + \|\bar{\mathcal{T}}_{\tilde{w}}(z)\|_F^2\,. \end{aligned} \quad (35)$$

Solve the minimization problem

$$\begin{aligned}\mathcal{H}_N &= \arg\min_{\mathcal{H}_N} \mathrm{tr}\mathbf{P} \\ &= \arg\min_{\mathcal{H}_N} \mathrm{tr}(\mathcal{B}_N\chi_m\mathcal{B}_N^T + \mathcal{W}_N\mathcal{Q}_N\mathcal{W}_N^T \\ &\quad + \mathcal{V}_N\mathcal{R}_N\mathcal{V}_N^T + \|\bar{\mathcal{T}}_{\tilde{x}}(z)\|_F^2 + \|\bar{\mathcal{T}}_{\tilde{w}}(z)\|_F^2) \end{aligned} \quad (36)$$

by considering $\frac{\partial}{\partial\mathcal{H}_N}\mathrm{tr}\,\mathbf{P} = 0$. Substitute $\mathbf{Q}$ and $\mathbf{R}$ with (7) and (8), arrive at (34), and complete the proof. ∎

Finally, compute the error matrix associated with (23) by

$$\begin{aligned}\mathbf{P} &= \mathcal{B}_N\chi_m\mathcal{B}_N^T + \alpha_\tau\mathcal{W}_N\mathcal{Q}_N\mathcal{W}_N^T + \beta_\tau\mathcal{V}_N\mathcal{R}_N\mathcal{V}_N^T \\ &\quad + \tilde{\mathbf{P}}_x + \tilde{\mathbf{P}}_w\,, \end{aligned} \quad (37)$$

where $\tilde{\mathbf{P}}_x = \tilde{\chi}_m^F$ and $\tilde{\mathbf{P}}_w = \|\bar{\mathcal{T}}_{\tilde{w}}(z)\|_F^2$.

5. Two-state Glucose Level Model

We now need to specify the uncertain matrices $\tilde{\mathbf{Q}}_N^{DT}$ and $\tilde{\mathbf{Q}}_N^T$ in (34) for timing jitter. For the two-state polynomial model, we write the system matrix $\mathbf{F}_k = \mathbf{F} + \Delta\mathbf{F}_k$ as

$$\mathbf{F}_k = \mathbf{F} + \tilde{\tau}_k\bar{\mathbf{F}}_k = \begin{bmatrix} 1 & \tau \\ 0 & 1 \end{bmatrix} + \tilde{\tau}_k\begin{bmatrix} 0 & 1 \\ 0 & 0 \end{bmatrix} \quad (38)$$

and the uncertain error ξ_k is given by (11).

To provide the averaging in $\tilde{\mathbf{Q}}_N^{DT}$ specified after (33), we start with $\tilde{\mathbf{D}}_{m,k} = \hat{\mathbf{F}}_N\mathbf{D}_{m,k}^{\Delta}$, where $\mathbf{F}_N$ is given by (14) and

$\mathbf{D}^{\Delta}_{m,k}$ by (18). For small jitter and other errors, we neglect the products of their values and obtain

$$\mathbf{D}^{\Delta}_{m,k} = \begin{bmatrix} \mathbf{0} & \mathbf{0} & \dots & \mathbf{0} & \mathbf{0} \\ \tilde{\tau}_{m+1}\bar{\mathbf{F}} & \mathbf{0} & \dots & \mathbf{0} & \mathbf{0} \\ \vdots & \vdots & \ddots & \vdots & \vdots \\ \tilde{\tau}_{k-1}\bar{\mathbf{F}}\mathbf{F}^{N-3} & \tilde{\tau}_{k-1}\bar{\mathbf{F}}\mathbf{F}^{N-4} & \dots & \mathbf{0} & \mathbf{0} \\ \tilde{\tau}_{k}\bar{\mathbf{F}}\mathbf{F}^{N-2} & \tilde{\tau}_{k}\bar{\mathbf{F}}\mathbf{F}^{N-3} & \dots & \tilde{\tau}_{k}\bar{\mathbf{F}} & \mathbf{0} \end{bmatrix} . \quad (39)$$

This gives $\bar{\tilde{\mathbf{D}}}_{m,k} = \bar{\hat{\mathbf{F}}}_N \mathbf{D}^{\Delta}_{m,k}$. Similarly we obtain $\tilde{\mathbf{T}}_{m,k} = \bar{\mathbf{H}}_N \hat{\mathbf{F}}_N \mathbf{D}^{\Delta}_{m,k}$ and arrive at $\tilde{\mathbf{Q}}^{DT}_N = \bar{\hat{\mathbf{F}}}_N \mathcal{Q}^{\Delta}_N \hat{\mathbf{F}}^T_N \bar{\mathbf{H}}^T_N$, where

$$\mathcal{Q}^{\Delta}_N = \mathcal{E}\{\mathbf{D}^{\Delta}_{m,k}\mathbf{W}_{m,k}\mathbf{W}^T_{m,k}\mathbf{D}^{\Delta^T}_{m,k}\} . \quad (40)$$

This gives $\tilde{\mathbf{Q}}^T_N = \bar{\mathbf{H}}_N \hat{\mathbf{F}}_N \mathcal{Q}^{\Delta}_N \hat{\mathbf{F}}^T_N \bar{\mathbf{H}}^T_N$.

Now, we assume that $\tilde{\tau}_k$, w_k, and v_k are small, zero mean, and mutually uncorrelated white Gaussian processes with the standard deviations σ_τ, σ_w, and σ_v, and first transform matrix $\mathbf{D}^{\Delta}_{m,k}$ as follows. The key product in (39) is $\bar{\mathbf{F}}\mathbf{F}^n = \begin{bmatrix} 1 \\ 0 \end{bmatrix}$. We thus assign a matrix $\tilde{\mathbf{T}}_n = \begin{bmatrix} \tilde{\tau}_n \\ 0 \end{bmatrix}$ and obtain

$$\mathbf{D}^{\Delta}_{m,k} = \begin{bmatrix} \mathbf{0} & \mathbf{0} & \dots & \mathbf{0} & \mathbf{0} \\ \tilde{\mathbf{T}}_{m+1} & \mathbf{0} & \dots & \mathbf{0} & \mathbf{0} \\ \vdots & \vdots & \ddots & \vdots & \vdots \\ \tilde{\mathbf{T}}_{k-1} & \tilde{\mathbf{T}}_{k-1} & \dots & \mathbf{0} & \mathbf{0} \\ \tilde{\mathbf{T}}_{k} & \tilde{\mathbf{T}}_{k} & \dots & \tilde{\mathbf{T}}_{k} & \mathbf{0} \end{bmatrix} . \quad (41)$$

Looking into (40), we notice that its key component is $\mathcal{E}\{\tilde{\tau}^2_k w^2_n\}$. Then for $X = \tilde{\tau}^2_k$ and $Y = w^2_n$ the Cauchy-Schwartz inequality $\mathcal{E}\{XY\} \leqslant \sqrt{\mathcal{E}\{X^2\}\mathcal{E}\{Y^2\}}$ gives $\mathcal{E}\{\tilde{\tau}^2_k w^2_n\} \leqslant \sqrt{\mathcal{E}\{\tilde{\tau}^4_k\}\mathcal{E}\{w^4_n\}}$. Since for Gaussian variables we have $\mathcal{E}\{\tilde{\tau}^4_k\} = 3\sigma^4_\tau$ and $\mathcal{E}\{w^4_k\} = 3\sigma^4_w$, after some transformations we obtain $\mathcal{Q}^{\Delta}_N \leqslant 3\sigma^2_\tau\sigma^2_w\mathbf{Q}^N_N$, where $\mathbf{Q}^N_N = \mathrm{diag}(\,\mathbf{J}_1\;\mathbf{J}_2\dots\mathbf{J}_N)$, in which $\mathbf{J}_i = \begin{bmatrix} i & 0 \\ 0 & 0 \end{bmatrix}$, $i \in [1, N]$.

The gain (34) can now be written as

$$\begin{aligned} \mathcal{H}_N \; = \; & (\mathbf{F}^{N-1}\chi_m\mathbf{H}^T_N + \alpha_\tau\bar{\mathbf{D}}_N\mathcal{Q}_N\mathbf{G}^T_N \\ & + 3\sigma^2_\tau\sigma^2_w\bar{\hat{\mathbf{F}}}_N\mathbf{Q}^N_N\hat{\mathbf{F}}^T_N\bar{\mathbf{H}}^T_N)(\mathbf{H}_N\chi_m\mathbf{H}^T_N \\ & + \alpha_\tau\mathbf{G}_N\mathcal{Q}_N\mathbf{G}^T_N + \beta_\tau\mathcal{R}_N \\ & + 3\sigma^2_\tau\sigma^2_w\bar{\mathbf{H}}_N\hat{\mathbf{F}}_N\mathbf{Q}^N_N\hat{\mathbf{F}}^T_N\bar{\mathbf{H}}^T_N)^{-1} . \end{aligned} \quad (42)$$

and we notice that under the assumption of small errors, the terms with $\sigma^2_\tau\sigma^2_w$ can be omitted and (42) becomes

$$\begin{aligned} \mathcal{H}_N \; = \; & (\mathbf{F}^{N-1}\chi_m\mathbf{H}^T_N + \alpha_\tau\bar{\mathbf{D}}_N\mathcal{Q}_N\mathbf{G}^T_N)(\mathbf{H}_N\chi_m\mathbf{H}^T_N \\ & + \alpha_\tau\mathbf{G}_N\mathcal{Q}_N\mathbf{G}^T_N + \beta_\tau\mathcal{R}_N)^{-1} . \end{aligned} \quad (43)$$

Note that, since the batch OFIR filtering estimate [27] can be computed iteratively using Kalman recursions [32], the batch (43) can also be computed using Kalman recursions. We finish the derivation of the robust H_2-OFIR filter with the iterative algorithm, which pseudo code is listed as Algorithm 1. The algorithm requires a maximized value $\max|\tilde{\tau}_k|$ of the time jitter in order for the estimate of the blood sugar level to be robust.

Algorithm 1: Robust H_2-OFIR Filtering Algorithm

Data: y_k, u_k, $\hat{x}_m$, P_m, Q, R, $\max|\tilde{\tau}_k|$

```
begin
    α_τ = (1 + max|τ̃_k| / τ) ;
    β_τ = (1 − max|τ̃_k| / τ) ;
    for k = 1, 2, ··· do
        m = k − N + 1 if k > N − 1 and m = 0
          otherwise;
        for i = m + 1, m + 2, ··· , k do
            P_k^- = F P_{k−1} F^T + α_τ B Q B^T ;
            S_k = H P_k^- H^T + β_τ R ;
            K_k = P_k^- H^T S^{−1} ;
            x̂_k = F x̂_{k−1} + K(y_k − H F x̂_{k−1}) ;
            P_k = (I − K_k H) P_k^- ;
        end for
    end for
    Result: x̂_k, P_k
end
```

5.1 Effect of Time Jitter on the Filter Performance

Analyzing (42), the following conclusions can be made. There are two types of corrections: the first-order corrections by the terms α_τ and β_τ and the second-order corrections by the terms $\sigma^2_\tau\sigma^2_w$. The fractional jitter $\bar{\delta}_\tau$ affects the blood sugar measurements in the opposite directions, as in (7) and (8), which is favorite for jitter reduction. The estimation error matrix (37) does not directly indicate the robustness of the H_2-OFIR filter, and the best is to prove the effect experimentally.

6. Glucose Monitoring in Diabetic Patients

In this section, we apply the filter designed to daily glucose measurements in diabetic patients. We use the above-considered two-state model and assume that all errors are Gaussian. Since the glucose measurement error reaches $\pm 20\%$ in the upper range, we set $\sigma_v = 20\,\mathrm{mg/dl}$. The scalar disturbance w_k is unknown, and we set σ_w that gives the best estimate for each smoothing window. We next consider the diabetes data available from [6]. Deliberately, we choose several databases related to monitoring at 8:00 before breakfast and apply a two-state UFIR smoother [33] on 3 days, one week, and two week horizons to obtain a pseudo ground truth. To investigate the blood sugar level dynamics, we use the H_2-OFIR, OFIR, Kalman, ML-FIR, and UFIR filters and minimize errors relative to the pseudo ground truth in the MSE sense.

The time jitter in “data-01” obtained over 134 days is shown in Fig. 1a. As we can see, the time variations are about ± 2 hours that corresponds to $\bar{\delta}_\tau = 3.79\%$. The daily glucose measurements, a pseudo ground truth obtained by 14-days smoothing, and the filtering estimates are sketched in Fig. 1b. First we notice that the robust H_2-OFIR filter produces the smallest RMSE of 19.78 mg/dl. The OFIR filter is less accurate (20.01 mg/dl), and the ML-FIR (28.00 mg/dl) and UFIR (27.92 mg/dl) filters give more errors.

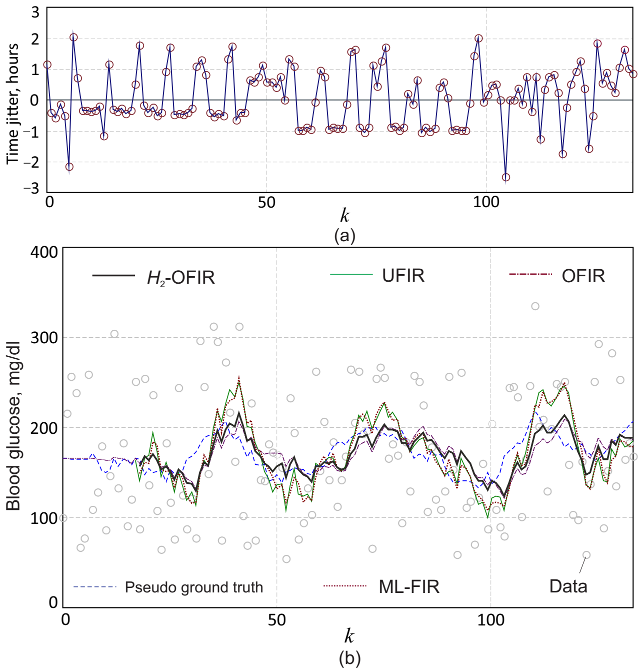

Fig. 1. Daily glucose measurements ("data-01") at 8.00 before breakfast in a diabetic patient: (a) timing jitter and (b) filtering estimates for a pseudo ground truth (14-days smoothed).

The time jitter in another "data-29" obtained over 148 days is shown in Fig. 2a. Instantly we notice that its mean is not

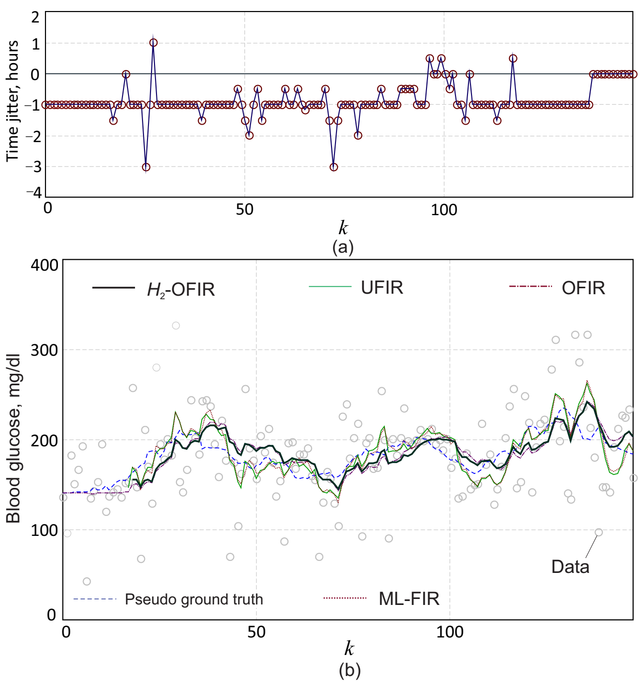

Fig. 2. Daily glucose measurements ("data-29") at 8.00 before breakfast in a diabetic patient: (a) timing jitter and (b) filtering estimates for a pseudo ground truth (14-days smoothed).

zero and that the time variations range from -3 to 1 hours that corresponds to $\bar{\delta}_\tau = 2.29\%$. The filtering estimates along with

TABLE I
ACCURACY IMPROVEMENT (IN %) BY ROBUST H_2-OFIR FILTER FOR DIFFERENT SMOOTHER WINDOWS AS FUNCTION ON THE FRACTIONAL TIME JITTER $\bar{\delta}_\tau$ (IN %)

δ_τ, %	3 days	7 days	14 days
3.79	0.224	0.143	1.144
4.77	5.362	4.014	4.581
9.53	8.044	8.223	9.161

a pseudo ground truth (14-days smoothing) are sketched in Fig. 2b. Again we notice that the robust H_2-OFIR filter gives the smallest RMSE (19.14 mg/dl), while the OFIR filter (19.22 mg/dl), UFIR (23.82 mg/dl), and ML-FIR (25.64 mg/dl) filters are less accurate.

Now we wonder how robust the H_2-OFIR filter is compared to the OFIR filter, which does not have the tuning option to mitigate timing jitter. To find out, we compute the difference between the H_2-OFIR and OFIR estimates, relate the result to the OFIR estimate, and plot in percents in Fig. 3. What

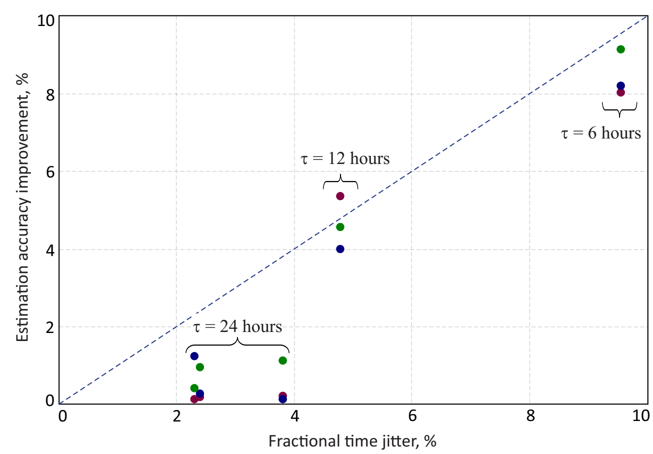

Fig. 3. Improvement of the OFIR filter accuracy (in %) by the robust H_2-OFIR filter as function of the fractional time jitter $\bar{\delta}_\tau$ (in %).

follows is that, for the maximum observed $\bar{\delta}_\tau = 3.8\%$ related to $\tau = 24$ hours, the filtering accuracy is improved only by 1.14%. Next, we assume that monitoring is conducted each $\tau = 12$ and $\tau = 6$ hours and infer that the estimation accuracy is improved proportionally to $\bar{\delta}_\tau$. Note that these projections do not accurately apply to glucose monitoring as blood sugar levels are higher during the day and lower at night. Nevertheless, it gives an idea of the effect of fractional time jitter on the accuracy of a robust filter. This is supported by Table I, from which we also deduce that the accuracy improvement does not depend on the smoother window.

Finally, we look at the estimated second state and compute the average rate of the blood sugar level. The most accurate robust H_2-OFIR filter reveals a low rate of 0.089 (mg/dl)/day in "data-01" and a high rate of 0.45 (mg/dl)/day in "data-29". Other rates obtained by different filters are listed in Table II.

TABLE II
BLOOD SUGAR LEVEL RATES IN (MG/DL)/DAY DETECTED IN "DATA-01" AND "DATA-29" BY DIFFERENT FILTERS

Data set	H_2-OFIR	OFIR	KF	ML-FIR	UFIR
"data-01"	0.089	0.058	0.103	0.039	0.129
"data-29"	0.451	0.449	0.557	0.271	0.418

7. Conclusions

To provide accurate monitoring of glucose level in diabetic patients under timing jitter caused by human factors, we have developed the robust *a posteriori* H_2-OFIR filter and compared its performance to the *a posteriori* OFIR filter. It turned out that under the maximum observed fractional daily jitter in glucose measurements of 4%, the accuracy improvement by the robust filter is less than 4%, which is small. In this case, the jitter can be ignored and the standard filters used. However, more frequent measurements result in larger fractional jitter that require robust estimates.

Acknowledgements

This work was supported by the Consejo Nacional de Ciencia y Tecnología (CONACyT) of Mexico Project A1-S-10287, Funding CB2017-2018.

References

[1] P. V. Balakrishnan, "On the problem of time jitter in sampling," *IRE Trans. Inform. Theory*, vol. 8, no. 3, pp. 226–236, 1962.

[2] E. Säckinger, *Analysis and design of transimpedance amplifiers for optical receivers*. Wiley, New York, 2017.

[3] *Jitter Specifications for Timing Signals: Renesas Electr. Corp. Application Note AN-840*. Renesas Electr. Corp., 2019.

[4] A. M. Raoufi, X. Tang, Z. Jing, X. Zhang, Q. Xu, and C. Zhou, "Blood glucose monitoring and its determinants in diabetic patients: a cross-sectional study in Shandong, China," *Diabetes Ther.*, vol. 9, no. 5, pp. 2055–2066, 2018.

[5] A. D. Association, "Classification and Diagnosis of Diabetes: Standards of medical care in diabetes," *Diabetes Ther.*, vol. 44, pp. S15–S33, 2021.

[6] M. M. Kahn, *Diabetes Data Set: UCI Machine Learning Repository https://archive.ics.uci.edu/ml/datasets/diabetes*, 1994.

[7] D. Wilson, "Convolution and Hankel operator norms for linear systems," *IEEE Trans. Autom. Contr.*, vol. 34, no. 1, pp. 94–97, 1989.

[8] K. Zhou, J. C. Doyle, and K. Glover, *Robust and Optimal Control*. Prentice-Hall, Upper Saddle River, NJ, 1996.

[9] P. L. Rawicz, P. R. Kalata, K. M. Murphy, and T. A. Chmielewski, "Explicit formiula for two state Kalman, H_2 and H_∞ Target tracking," *IEEE Trans. Aero. Electr. Syst.*, vol. 39, no. 1, pp. 53–69, 2003.

[10] N. Narasimhamurthi, "Estimating the parameters of a sinusoid sampled by a clock with accumulated jitter," in *IEEE Instrum. Meas. Techn. Conf.* IEEE, Ottawa, Canada, May 1997, 1997, pp. 1132–1135.

[11] N. C. Georghiades and D. L. Snyder, "The expectation maximization algorithm for symbol unsynchronized sequence detection," *IEEE Trans. Commun.*, vol. 39, no. 1, pp. 54–61, 1991.

[12] F. Eng and F. Gustafsson, "Identification with stochastic sampling time jitter," *Automatica*, vol. 44, no. 3, pp. 637–646, 2008.

[13] X. G. Guo and G. Yang, "Insensitive h_∞ filtering for fast-sampled linear systems with respect to sampling time jitter," in *24th Chinese Contr. Dec. Conf. (CCDC)*. Taiyuan, China, May 2012, 2012, pp. 4202–4207.

[14] L. Xie, Y. C. Soh, C. Du, and Y. Zou, "Robust H_2 estimation and control," *J. Contr. Theory Appl.*, vol. 2, pp. 20–26, 2004.

[15] L. Xie, "On robust H_2 estimation," *Acta Automat. Sinica*, vol. 31, no. 1, pp. 1–12, 2005.

[16] M. Souza, A. R. Fioravanti, and J. C. Geromel, "H_2 sampled-data filtering of linear systems," *IEEE Trans. Signal Process.*, vol. 62, no. 18, pp. 4839–4846, 2014.

[17] B. Hassibi, A. H. Sayed, and T. Kailath, *Indefinite-quadratic estimation and control: a unified approach to H^2 and H^∞ theories*. SIAM, Philadelphia, 1999.

[18] K. Z. Liu and T. Sato, "Lmi solution to singular h_2 suboptimal control problems," in *14th World Congress of IFAC*. Beijing, China, July 1999, 1999, pp. 3011–3016.

[19] Z. Tan, Y. C. Soh, and L. Xie, "Envelope-constrained H_2 FIR filter design," *Circ. Syst. Signal Process.*, vol. 18, no. 6, pp. 539–551, 1999.

[20] B. S. Chen and J. C. Hung, "Fixed-order H_2 and H_∞ optimal deconvolution filter designs," *Signal Process.*, vol. 80, no. 2, pp. 311–331, 2000.

[21] S. Wang, L. Xie, and C. Zhang, "H_2 optimal inverse of periodic FIR digital filters," *IEEE Trans. Signal Process.*, vol. 48, no. 9, pp. 2696–2700, 2000.

[22] ——, "Mixed H_2/H_∞ deconvolution of uncertain periodic FIR channels," *Signal Process.*, vol. 81, no. 10, pp. 2089–2103, 2001.

[23] W. H. Kwon and S. Han, *Receding horizon control: model predictive control for state models*. Springer, London, 2005.

[24] Y. S. Lee, S. H. Han, and W. H. Kwon, "H_2/H_∞ FIR for discrete-time state space models," *Int. J. Contr. Autom. Syst.*, vol. 4, no. 5, pp. 645–652, 2006.

[25] C. K. Ahn, S. Zhao, Y. S. Shmaliy, and H. Li, "On the $\ell_2 - \ell_\infty$ and H_∞ performance of the continuous-time deadbeat H_2 FIR filter," *IEEE Trans. Circ. Syst. II Express Briefs*, vol. 65, no. 11, pp. 1798–1802, 2018.

[26] Y. S. Shmaliy, "Linear optimal FIR estimation of discrete time-invariant state-space models," *IEEE Trans. Signal Process.*, vol. 58, no. 6, pp. 3086–3096, 2010.

[27] Y. S. Shmaliy and O. Ibarra-Manzano, "Time-variant linear optimal finite impulse response estimator for discrete state-space models," *Int. J. Adapt. Contr. Signal Process.*, vol. 26, no. 2, pp. 95–104, 2012.

[28] S. Zhao and Y. S. Shmaliy, "Unified maximum likelihood form for bias constrained FIR filters," *IEEE Signal Process. Lett.*, vol. 23, no. 12, pp. 1848–1852, 2016.

[29] Y. S. Shmaliy, "An iterative Kalman-like algorithm ignoring noise and initial conditions," *IEEE Trans. Signal Process.*, vol. 59, no. 6, pp. 2465–2473, 2011.

[30] Y. S. Shmaliy, S. Zhao, and C. K. Ahn, "Unbiased FIR filtering: an iterative alternative to Kalman filtering ignoring noise and initial conditions," *IEEE Contr. Syst. Mag.*, vol. 37, no. 5, pp. 70–89, 2017.

[31] J. Ortega-Contreras, E. Pale-Ramon, Y. S. Shmaliy, and Y. Xu, "A novel approach to H_2 FIR prediction under disturbances and measurement errors," *IEEE Signal Process. Lett.*, vol. 28, pp. 150–154, 2021.

[32] S. Zhao, Y. S. Shmaliy, and F. Liu, "Optimal FIR filter for discrete-time LTV systems and fast iterative algorithm," *IEEE Trans. Circ. Syst. II, Express Briefs*, vol. 68, no. 4, pp. 1527–1531, 2021.

[33] Y. S. Shmaliy and L. Morales-Mendoza, "FIR smoothing of discrete-time polynomial models in state space," *IEEE Trans. Signal Process.*, vol. 58, no. 5, pp. 2544–2555, 2010.

Creative Commons Attribution License 4.0 (Attribution 4.0 International, CC BY 4.0)

This article is published under the terms of the Creative Commons Attribution License 4.0
https://creativecommons.org/licenses/by/4.0/deed.en_US